

Load Capacity and Field Assessments of Concrete Bridge before Strengthening

Haleem K. Hussain^{*1}, Liu Gui Wei², Mudhar Hasan Gatea³

^{*1}*Basrah University, College of Engineering, Civil Engineering Department, Basrah City, Iraq*

²*School of transportation science and Engineering /Bridge and Tunnel Engineering*

Dep. /Harbin Institute of Technology/. Harbin City/China, [150090]

³*Basrah University, College of Engineering, Civil Engineering Department, Basrah City, Iraq*

Abstract:- Bridge failures are often observed due different reasons, such as environmental sever conditions, exceed the traffic load, poor initial design requirements, etc; as well as the unexpected disaster accidents such as earthquakes, As a result, evaluation of the stability of bridge abutments has become an important part of engineering research. This study present the whole inspection process of the Zhong Xing Bridge including the main beam , support, deck system (pavement, drainage , side walk and railing guard), pier, reinforcement protect layer and corrosion and the abutment (ear walls, cone slope and foundation). The investigation showing the bridge has minor defects through the substructures while the super structure consist of the T-beam girders section parts. The data showing the T-beam have no enough reservoir capacity and need to strengthening, while the other parts in a good condition and meet the design requirements. This research also proposed design strengthening method of bridge.

Keywords:- Field investigation, concrete T-Beam girder, site inspection, Zhong Xing Bridge.

I. INTRODUCTION

There are several situations in which a civil structure would require strengthening or rehabilitation due to lack of strength, stiffness, ductility and durability.

Bridges can be considered structurally deficient if significant load capacity is found to be in poor or bad conditions because of deterioration or damage. The facts that a bridge is structurally deficient does not meet the standard requirements that it is likely to be is unsafe. Bridges are considered functionally out of date when the geometry of the road no longer meets the minimum design specification.

The sufficiency rating or damage level of a bridge can be classified between 0 (low) to 100 (high), based on bridge conditions, geometry, traffic, the condition of waterway passes underneath the bridge. Any way the low sufficiency rating does not mean the bridge is unsafe or immediately need repair.

The problem of corrosion deterioration of concrete bridges was first identified in United States in early 1960's (Richard et al.). The ultimate strength and material properties of concrete like strength and modulus of elasticity estimated from Non Destructive tests can vary from actual values and load tests as well as NDT data can be used for assessment purposes (Jaroslav et al. 2002) [1].

Doebling et al. [2] have presented a comprehensive review on damage detection from vibration characteristics. An important problem in this area of research is to detect the local damage using structural responses under operational moving loads. Lee et al. [3] studied the identification of the operational modal properties of a bridge structure under traffic loading and carried out the condition assessment based on the estimated modal parameters. Static and dynamic responses were used to identify local damages in plate- like structure [4]. Time frequency analysis is also used for the detection of cracks in a beam and gear and roller system [5]. A strategy based on energy change [6] was proposed for damage detection with long-span bridges.

Corrosion induced deterioration of RC structures, especially bridges, due to frequently applied deicing salts, is a main challenge to civil asset managers worldwide. Corrosion affects the reliability of RC structures, both in strength and serviceability limit states. In the past decade, many researchers worldwide have proposed various reliability based maintenance management systems. In these systems, mechanistic deterioration models are utilized in a probabilistic framework to account for temporal variations in material properties and loads as random variables [7].

In most bridge management systems, routine inspections are mandatory, biannually. This is not only an expensive approach, but also in some congested traffic regions or severe environments, more frequent inspections may be necessary during the lifetime of the bridge. Suo and Stewart [8] showed the usage of data gathered during inspections in the updating of reliability models.

Haleem et al [9] describes and evaluates the state of Qing Shang Bridge. The deterioration of bridge can be occurred due to increased internal forces led to higher loading and due to sever climatic and

environmental weathers changes, bridges need reinforcement because damage due to external factors which reduced the cross-sectional resistance to external loads.

II. BRIDGE OVERVIEW

The technical condition of the Zhong Xing Bridge structures was checked. The inspection include following; main beam, supports, deck system (pavement, expansion joints, drainage, sidewalks and railings), abutments, piers, concrete strength, reinforced concrete protective layers and steel corrosion.

Zhong Xing bridge is located in the G221 National Highway (Harbin – Tong Jiang Road) at the Da Lou Mi town /China , bridge length 96 meters, 4 spans, simply supported of 20-meter reinforced concrete T beam layout of $8.0 + 4 \times 20.0 + 8.00$, the T-shaped main beam has connected laterally with rigid connection. Deck width is $7 + 2 \times 1.75\text{m}$ sidewalk, design load criteria of the two levels, vehicle No.-15, and truck No. 80. The environmental categories is II, deck longitudinal slope of 1.0%, the transverse deck cross slope: 2.0% of two-lane, the reinforced concrete T-beam using R25 concrete type and reinforced concrete piers and abutments were R20 concrete type. The bridge was built in 1982 has been used for about 30 years ago.

III. GENERAL DESCRIPTION

The reinforcement and renovation process project was carried on the Zhong Xing Highway River Bridge. General views of bridge are shown in Fig. (1).



Fig. (1) Zhong Xing Bridge

The original design deck is 10cm thick cement concrete pavement. In 2009 the original cement concrete deck pavement affixed asphalt concrete pavement, thickness 8cm. The support bed is a flat bed rubber bearing, bearing dimensions of $20.0 \times 20.0 \times 2.8\text{cm}$;

The Zhong Xing Bridge general layout, structural details of bridge superstructure and bridge substructure elements details are shown in Fig. (2) and Fig. (3).

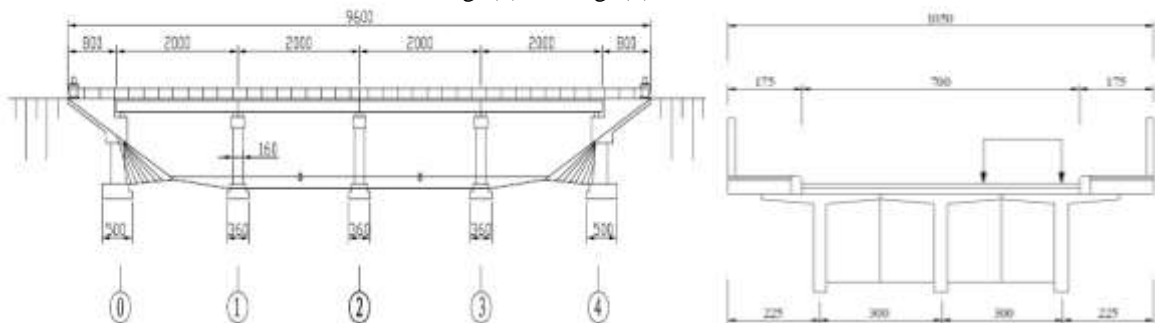


Fig. (2) bridge details (cm).

In recent years, with the excessive increasing of large vehicles and riverbed sand mining, and due to adverse factors, the bridge has cracks in the main load-bearing structure, concrete shed, deck leakage as well as bridge pier foundation exposed to erosion effects. The Heilongjiang Provincial Highway Administration gave authorized to the Experimental Center of Harbin Institute of Technology Transportation to inspect the technical condition of the main structure of Zhong Xing Bridge and its subsidiary structures

The bridge has cracks in the main load-bearing structure, the main beam concrete of bridge, surface leaks, cracks, the exposed tendons as well as the pier foundation have erosion exposed a variety of deterioration. Major inspection was conventional visual inspection of bridges, bridge special detection, as well as static and dynamic load test for bridge structural member shows defect condition, according to the Ministry of Transportation Highway Bridges and culverts Standards (JIG H11-2004) [10].

The test results showed that the technical requirements of the technical conditions of the active duty Zhong Xing Bridge is already less than the original design requirements. In order to ensure the safe operation of the Zhong Xing Bridge and extend the service life time, it is recommended to urgently adopt technical measures to reinforce and modify the loading bridge capacity and keep it work safely.

IV. INSPECTION BRIDGE PARTS

3.1 Expansion Joints

The asphalt overlay was designed and implemented with a continuous deck expansion joints. The field inspection shows damaged pavement and expansion joints structure, due to the expose asphalt overlay concrete deck to sever conditions which led to serious damage and that reflecting induced cracking. Five asphalt concrete expansion joints generally broken. Typical failure conditions as shown in Fig. (8).

3.2 Sidewalk and Guardrail

The bridge guardrail is a reinforced concrete columns and steel tube combination; columns are fixed in the top surface of the flange plate T beam. Often appear in nearly three decades, using the sidewalk causing destroyed of guardrail as well as du to other car accidents. The site inspection of guardrail damaged results are presents that the steel the concrete column was peel off more than 80%, steel of column are corroded and concrete cover was more than 30% the ends of column between the steel tubs lost about 40% of all, and beam end between pillars steel section is missing more than 30 %.

3.3 Bridge Ends Inspection

Fig. (10) shows the side wall with the abutment back wall connection, no obvious damage fracture, short local presence fine cracks and its maximum width of approximately 0.1mm.



Fig. (10) Wing walls and ear wall damaged condition

The site inspection results show that during the wet period washout lead to large defect of abutment truncated cone and also paving defects and other undesirable phenomena. The typical failure condition is shown in Fig. (11).

The state of abutment back wall concrete structure has admissibility cracks, exposed tendons, frost damage, etc. Defects also include cone slope protection. Abutment based on the basic integrity of overlying soil and no exclusive symptoms.

3.4 Pier inspection

Since the bridge exposed to water flow of river over 30 years ago, the pier was suffering from different damage levels. Furthermore, the concrete gravel was exposed due these reasons and other undesirable phenomena. Smooth and fine cracks exit on the pier body, maximum crack width about 0.1mm. Fig. (12) shows the pier condition.



Fig. (11) Peel of the cement mortar and exposed gravels of pier condition

3.5 Substructure member

Ordinary reinforced concrete beam is simply supported T-beam is the main bridge girder. The clear span 19.5 meters.

3.5.1 Crack Inspection

The main beam No. 1 and No. 3 (left and right side of the bridge) are prevalent in the mid-span about 2 meters within a through T beams rib, crack spacing lies between 20 – 50 cm, most common about 25 cm spacing. Crack pattern showed the upper part were narrow while lower parts have larger crack width due to flexural tensile effects. The width cracks distribution was between 0.1mm ~ 0.28 mm and crack width exceeding 0.25mm only at vertical crack. The longest crack was at the beam rib has been extended to the flange of the beam, about 1.5 meters length. Fig. (17) shows the cracks pattern.



Fig. (17) Bending and diagonal tensile cracks pattern.

3.5.2 Diaphragm beam inspection

Two set intermediate diaphragm was installed at left and right ends of the beam, a total is four diaphragm beams. They are made of a rigid connection monolithically poured with main beam girder. The field investigation found no structural cracks and corrosion, concrete cover have damaged. Fig. (19) show that all diaphragm beam in a good condition.



Fig. (19) Diaphragm beam conditions detailed

3.5.3 Flange Plate

The field survey showed that the main T- beam flange, web and diaphragm beam were whole cast at same time during the construction process, Therefore there is no crack and local leakage which can causes whitened area as shown in Fig. (20).

However, the flange plate exposed to the direct effect of cyclic loading and large area of flange plate have cracks, water seepage whitened as well as frozen which lead to a reinforced fall off the concrete cover causing steel corrosion. However these defects will lead to reduce the section capacity.



Fig. (20) The flange cracks, water seepage whitened condition and steel corrosion.

3.6. Compressive strength of concrete.

Concrete strength testing can directly reflect the quality of the concrete of the structure, according to the evaluation of the (Rebound assessment of concrete compressive strength Technical Specification-Chinese Standards JGJ/T23-92) [11]. The superstructure, piers and other components were tested.

Test surface and the angle correction for non-level state survey area. Table (2), Table (3), Table (4), and Table (5) listed, respectively, for the upper structure (main beam), the piers and abutments test results.

Table (2) Rebound test results of main concrete beam No.1.

| Item | | Point No. 1 | Point No. 2 | Point No. 3 | Point No. 4 | Point No. 5 | Point No. 6 |
|-------|----|-------------|-------------|-------------|-------------|-------------|-------------|
| Point | 1 | 38 | 42 | 48 | 48 | 50 | 42 |
| | 2 | 44 | 46 | 42 | 40 | 48 | 50 |
| | 3 | 42 | 48 | 36 | 48 | 52 | 44 |
| | 4 | 42 | 48 | 36 | 44 | 48 | 50 |
| | 5 | 38 | 42 | 42 | 42 | 48 | 52 |
| | 6 | 40 | 48 | 48 | 50 | 43 | 42 |
| | 7 | 44 | 30 | 38 | 48 | 36 | 38 |
| | 8 | 48 | 36 | 42 | 50 | 38 | 43 |
| | 9 | 44 | 42 | 44 | 42 | 43 | 38 |
| | 10 | 46 | 44 | 30 | 42 | 43 | 43 |
| | 11 | 48 | 36 | 42 | 46 | 42 | 38 |
| | 12 | 46 | 43 | 42 | 52 | 43 | 44 |
| | 13 | 48 | 46 | 42 | 42 | 42 | 42 |
| | 14 | 42 | 46 | 32 | 42 | 42 | 42 |
| | 15 | 50 | 43 | 48 | 42 | 42 | 43 |
| | 16 | 52 | 43 | 50 | 48 | 44 | 46 |
| Point | 1 | 44 | 42 | 42 | 48 | 48 | 42 |
| | 2 | 42 | 46 | 36 | 48 | 48 | 44 |
| | 3 | 42 | 42 | 42 | 44 | 43 | 43 |
| | 4 | 44 | 42 | 38 | 42 | 43 | 43 |
| | 5 | 48 | 44 | 42 | 48 | 43 | 43 |
| | 6 | 44 | 43 | 44 | 46 | 42 | 44 |
| | 7 | 46 | 46 | 42 | 48 | 43 | 42 |
| | 8 | 48 | 46 | 42 | 42 | 42 | 42 |
| | 9 | 46 | 43 | 42 | 42 | 42 | 43 |
| | 10 | 42 | 43 | 84 | 48 | 44 | 46 |

Table (3) Pier concrete rebound test results.

| Item | Abutment | | | Pier No.1 | | | |
|-------|-------------|-------------|-------------|-------------|-------------|-------------|----|
| | Point No. 1 | Point No. 2 | Point No. 3 | Point No. 4 | Point No. 5 | Point No. 6 | |
| Point | | 44 | 38 | 40 | 42 | 40 | 38 |
| | | 42 | 34 | 33 | 38 | 34 | 38 |
| | | 41 | 41 | 39 | 36 | 38 | 44 |
| | | 40 | 38 | 40 | 38 | 42 | 46 |
| | | 38 | 41 | 41 | 36 | 44 | 40 |
| | | 41 | 36 | 39 | 42 | 42 | 46 |
| | | 32 | 39 | 45 | 42 | 36 | 46 |
| | | 32 | 39 | 45 | 42 | 36 | 46 |
| | | 38 | 43 | 34 | 44 | 38 | 48 |
| | 10 | 42 | 42 | 41 | 44 | 46 | 38 |
| | 11 | 38 | 42 | 40 | 42 | 48 | 42 |
| | 12 | 42 | 39 | 39 | 42 | 38 | 40 |
| | 13 | 32 | 38 | 43 | 44 | 42 | 44 |
| | 14 | 40 | 32 | 38 | 42 | 50 | 42 |
| | 15 | 38 | 40 | 39 | 40 | 40 | 48 |
| | 16 | 32 | 39 | 34 | 38 | 40 | 46 |

| | | | | | | | |
|-------|----|----|----|----|----|----|----|
| Point | 1 | 41 | 38 | 40 | 38 | 40 | 44 |
| | 2 | 40 | 41 | 39 | 38 | 38 | 40 |
| | 3 | 39 | 38 | 40 | 42 | 42 | 46 |
| | 4 | 41 | 41 | 41 | 42 | 42 | 46 |
| | 5 | 38 | 39 | 39 | 44 | 42 | 44 |
| | 6 | 40 | 38 | 41 | 44 | 38 | 42 |
| | 7 | 38 | 39 | 40 | 42 | 40 | 40 |
| | 8 | 38 | 38 | 39 | 42 | 42 | 44 |
| | 9 | 40 | 40 | 38 | 42 | 40 | 42 |
| | 10 | 38 | 39 | 39 | 40 | 40 | 46 |

Table (4) Rebound test results of main beams concrete

| Item | Main Beam No. 2 | | | Main Beam No. 3 | | |
|-------|-----------------|-------------|-------------|-----------------|-------------|-------------|
| | Point No. 1 | Point No. 2 | Point No. 3 | Point No. 4 | Point No. 5 | Point No. 6 |
| point | 1 | 40 | 41 | 43 | 43 | 38 |
| | 2 | 42 | 41 | 45 | 45 | 41 |
| | 3 | 41 | 39 | 41 | 39 | 31 |
| | 4 | 43 | 38 | 46 | 39 | 38 |
| | 5 | 45 | 42 | 40 | 38 | 40 |
| | 6 | 40 | 38 | 39 | 38 | 34 |
| | 7 | 39 | 43 | 35 | 40 | 39 |
| | 8 | 39 | 38 | 32 | 42 | 38 |
| | 9 | 32 | 40 | 39 | 39 | 32 |
| | 10 | 34 | 41 | 38 | 35 | 41 |
| | 11 | 38 | 38 | 39 | 38 | 34 |
| | 12 | 33 | 32 | 45 | 37 | 40 |
| | 13 | 39 | 31 | 34 | 40 | 44 |
| | 14 | 40 | 32 | 40 | 32 | 41 |
| | 15 | 42 | 38 | 41 | 41 | 38 |
| | 16 | 39 | 39 | 38 | 38 | 44 |
| point | 1 | 40 | 41 | 41 | 39 | 38 |
| | 2 | 41 | 39 | 40 | 39 | 41 |
| | 3 | 40 | 38 | 39 | 38 | 38 |
| | 4 | 39 | 38 | 39 | 38 | 40 |
| | 5 | 39 | 38 | 38 | 40 | 39 |
| | 6 | 38 | 49 | 39 | 39 | 38 |
| | 7 | 39 | 41 | 41 | 38 | 41 |
| | 8 | 40 | 38 | 41 | 40 | 40 |
| | 9 | 42 | 38 | 38 | 41 | 41 |
| | 10 | 39 | 39 | 41 | 38 | 38 |

According to (Rebound method to assess the compressive strength of concrete standard specification (JGJ/T23-92) [11], the averages of each measurement area, intensity standard deviation, as well as concrete strength estimation value, were computing respectively, by the following formula:

$$\begin{aligned}
 m_{f_{cu}^c} &= \left(\sum_{i=1}^n f_{cu,i}^c \right) / n \\
 S_{f_{cu}^c} &= \sqrt{\sum_{i=1}^n (f_{cu,i}^c)^2 - n(m_{cu,i}^c)^2} / (n-1) \\
 f_{cu,e} &= m_{f_{cu}^c}^c - 1.645 f_{cu}^c
 \end{aligned}$$

Where:

$m_{f_{cu}^c}$

f_{cu}^c : The average value of the converted value of the measurement area concrete strength (MPa), accurate to 0.1MPa

n : For a single detection component, take a member of the survey area number; batch testing components, take and sampling the member survey area number;

 $f_{cu,e}$

$f_{cu,e}$: Standard deviation of the strength of concrete conversion value of the structure or components measured areas, (accurate to 0.01MPa).

Table 5 Rebound test result of main girder concrete strength value (unit: MPa)

| Item | Main Beam | | Abutment | | Pier No. 1 | | Pier No. 2 | | Pier No. 3 | | |
|--------------------|----------------|--------------------------------|----------------|--------------------------------|----------------|--------------------------------|----------------|--------------------------------|----------------|--------------------------------|------|
| | Rebound values | Revised intensity values (MPa) | |
| Test Data | 1 | 44.0 | 30.2 | 41 | 26.2 | 38 | 22.6 | 40 | 25 | 39 | 23.8 |
| | 2 | 42.0 | 27.5 | 40 | 25.0 | 38 | 22.6 | 41 | 26.2 | 39 | 23.8 |
| | 3 | 42.0 | 27.5 | 39 | 23.8 | 42 | 27.5 | 40 | 25.0 | 38 | 22.6 |
| | 4 | 44.0 | 30.2 | 41 | 26.2 | 42 | 27.5 | 39 | 23.8 | 38 | 22.0 |
| | 5 | 48.0 | 36.0 | 38 | 22.6 | 44 | 30.2 | 39 | 23.8 | 40 | 25.0 |
| | 6 | 44.0 | 30.2 | 40 | 25.0 | 44 | 30.2 | 38 | 22.6 | 39 | 23.8 |
| | 7 | 46.0 | 33.0 | 38 | 22.6 | 42 | 27.5 | 39 | 23.8 | 38 | 22.6 |
| | 8 | 48.0 | 36.0 | 38 | 22.6 | 42 | 27.5 | 40 | 25 | 40 | 25.0 |
| | 9 | 46.0 | 33.0 | 40 | 25.0 | 42 | 27.5 | 42 | 27.5 | 41 | 26.2 |
| | 10 | 42.0 | 27.5 | 38 | 22.6 | 40 | 25.0 | 39 | 23.8 | 38 | 22.6 |
| | 11 | 42.0 | 27.5 | 38 | 22.6 | 40 | 25.0 | 41 | 26.2 | 38 | 22.6 |
| | 12 | 46.0 | 33.0 | 41 | 26.2 | 38 | 22.6 | 39 | 23.8 | 41 | 26.2 |
| | 13 | 42.0 | 27.5 | 38 | 22.6 | 42 | 27.5 | 38 | 22.6 | 38 | 22.6 |
| | 14 | 42.0 | 27.5 | 41 | 26.2 | 42 | 27.5 | 38 | 22.6 | 40 | 25.0 |
| | 15 | 44.0 | 30.2 | 39 | 23.8 | 42 | 27.5 | 38 | 22.6 | 39 | 23.8 |
| | 16 | 42.0 | 27.5 | 38 | 22.6 | 38 | 22.6 | 40 | 25.0 | 38 | 22.6 |
| | 17 | 46.0 | 33.0 | 39 | 23.8 | 40 | 25.0 | 41 | 26.2 | 41 | 26.2 |
| | 18 | 46.0 | 33.0 | 38 | 22.6 | 42 | 27.5 | 38 | 22.6 | 40 | 25.0 |
| | 19 | 40.0 | 25.0 | 40 | 25.0 | 40 | 25.0 | 38 | 22.6 | 41 | 26.2 |
| | 20 | 43.0 | 28.8 | 39 | 23.8 | 40 | 25.0 | 39 | 23.8 | 38 | 22.6 |
| | 21 | 42.0 | 27.5 | 40 | 25.0 | 44 | 30.2 | 41 | 26.2 | 40 | 25.0 |
| | 22 | 45.0 | 31.6 | 39 | 23.8 | 40 | 25.0 | 40 | 25.0 | 41 | 26.2 |
| | 23 | 42.0 | 27.5 | 40 | 25.0 | 46 | 33.0 | 39 | 23.8 | 38 | 22.6 |
| | 24 | 38.0 | 22.6 | 41 | 26.2 | 46 | 33.0 | 39 | 23.8 | 40 | 25.0 |
| | 25 | 42.0 | 27.5 | 39 | 23.8 | 44 | 30.2 | 38 | 22.6 | 38 | 22.6 |
| | 26 | 44.0 | 30.2 | 41 | 26.2 | 42 | 27.5 | 39 | 23.8 | 40 | 25.0 |
| | 27 | 42.0 | 27.5 | 40 | 25.0 | 40 | 25.0 | 40 | 25.0 | 39 | 23.8 |
| | 28 | 42.0 | 27.5 | 39 | 23.8 | 44 | 30.2 | 41 | 26.2 | 38 | 22.6 |
| | 29 | 42.0 | 27.5 | 38 | 22.6 | 42 | 27.5 | 38 | 22.6 | 37 | 21.5 |
| | 30 | 48.0 | 36.0 | 39 | 23.8 | 46 | 33.0 | 41 | 26.2 | 38 | 22.6 |
| Measured points | | 30 | | 30 | | 30 | | 30 | | 30 | |
| Average | | 30.2 | | 24.2 | | 27.3 | | 24.3 | | 23.9 | |
| Standard Deviation | | 2.84 | | 1.35 | | 2.66 | | 1.8 | | 1.8 | |
| Estimated Value | | 25.5 | | 22.0 | | 22.9 | | 21.3 | | 20.9 | |

Based on the rebound test method of the upper structure (main beam), piers and abutments strength of concrete degree (estimated value) meet the design requirements.

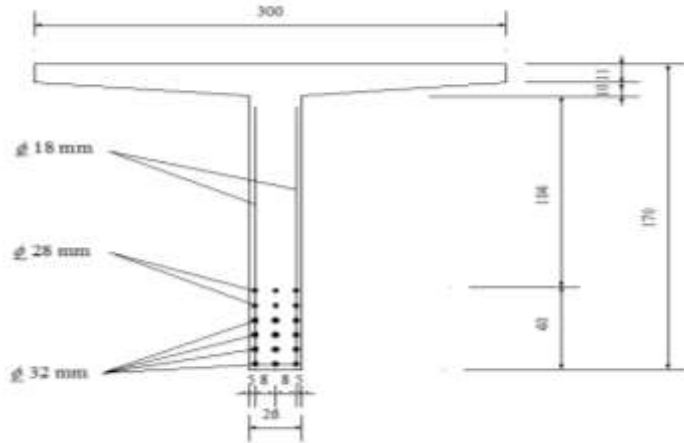


Fig. (22) Cross-section reinforced beam layout (unit cm).

The main beam longitudinal bar diameter is 12φ32mm and 6φ28mm, and the diameter of the stirrup φ18mm; the average concrete beam cover at bottom was 29.1mm, and at the side of around 25.1mm. Fig. (22) showing beam reinforcement details.

3.7 Rebar Corrosion Detection

The harmful substances intrusion concrete, will affect the durability of the structure, the protective layer of concrete erosion by CO₂ could be reach to the steel surface to reduce the alkalinity around the reinforced concrete, high chloride ion intrusion reinforced form Oxide film on the steel surface can cause damage, so that the intrusion chloride ion into reinforced concrete and available of Oxygen and moisture , harmful corrosion will affect the reinforcements steel which reflect reduction of cross-sectional area, and generated expanded material which undesirable inside the concrete surrounding the steel bars, eventually leading to breaking of the concrete structure badly.

The potentiometric method is the one of method to detect the reinforcement corrosion caused by the potential changes. The potential measurements changes are caused by the use of concrete reinforcement corrosion potential reaction. Four survey areas were arranged in the main beam, abutments and piers to determination of steel corrosion conditions by measuring the Reinforced potential situation. The test results are as listed in Table (7).

Table (7) steel corrosion test results (Unit: mv).

| Item | The measured data of the steel corrosion | | | | |
|------------------|--|-----|-----|-----|-----|
| Main Beam | -12 | -13 | -4 | -3 | -2 |
| | -3 | -3 | -2 | -1 | -10 |
| | -9 | -4 | -2 | -3 | -3 |
| | -12 | -3 | -13 | -6 | -4 |
| | -2 | -4 | -5 | -13 | -12 |
| | -24 | -13 | -4 | -3 | -16 |
| | -4 | -3 | -6 | -9 | -5 |
| Pier | -3 | -1 | -1 | -3 | -8 |
| | -13 | -8 | -2 | -3 | -6 |
| | -3 | -12 | -4 | -2 | -3 |
| | -2 | -6 | -1 | -3 | -3 |
| | -14 | -2 | -3 | -7 | -2 |
| | -10 | -11 | -8 | -4 | -3 |

According to the field test results, and standard of Highway Bridges Carrying Capacity Detection Assessment Procedures, reinforced potential conditions specified in relationship with steel corrosion show that the bridge reinforced steel corrosion or steel corrosion activity is not clear.

3.8 Evaluation of Bridge Assessments

According to bridge inspection field results, and with refereeing of standard of highway bridges and culverts specification (JTG H11-2004) [12], the technical condition rating of the bridge (Dr) calculated as follows:

$$D_r = 100 - \frac{(\sum_{i=1}^{17} R_i - W_i)}{5}$$

Where:

R_i : Assessment Scale;

W_i : The right degree.

The bridge technical evaluations of the results are listed in Table 8.

Table 8 Bridge technical condition rating

| Item | Part | Area damage degree | Using functional influence | Development correction | Assessment scale R_i | Weights W_i | Score |
|------------------|--|--------------------|----------------------------|------------------------|------------------------|---------------|-------|
| 1 | Wing Wall, Ear Wall | 0 | 0 | 0 | 0 | 1 | 0 |
| 2 | Cone Slope, Protection Slope | 2 | 1 | 1 | 4 | 1 | 4 |
| 3 | Abutment and Base | 1 | 1 | 0 | 2 | 23 | 46 |
| 4 | Piers and foundation | 1 | 1 | 0 | 2 | 24 | 48 |
| 5 | Foundation erosion | 2 | 2 | 1 | 5 | 8 | 40 |
| 6 | Supports | 0 | 0 | 0 | 0 | 3 | 0 |
| 7 | The upper part of the main Load-bearing structure | 1 | 2 | 1 | 4 | 20 | 80 |
| 8 | The upper part of the general Load-bearing structure | 1 | 1 | 1 | 3 | 1 | 3 |
| 9 | Bridgehead Bump | | | | | | |
| 10 | Deck Pavement | 2 | 2 | 1 | 5 | 3 | 15 |
| 11 | Expansion joints | 2 | 2 | 1 | 5 | 3 | 15 |
| 12 | Sidewalk | 1 | 1 | 1 | 3 | 1 | 3 |
| 13 | Railing, guardrail | 2 | 2 | 1 | 5 | 1 | 5 |
| 14 | Lighting, signs | 0 | 0 | 0 | 0 | 1 | 0 |
| 15 | Drainage system | 0 | 0 | 0 | 0 | 1 | 0 |
| 16 | Modulating structures | 0 | 0 | 0 | 0 | 3 | 0 |
| Dr | | 44.2 | | | | | |
| Technical graded | | Class No. III | | | | | |

The higher values of Dr indicate that the structure have better technical condition. The evaluation results of the structural bridge elements according to the specification can be illustrate as follows:

$D_r \geq 88$: Class I, need normal maintenance;

$88 > D_r \geq 60$: Class II, and need of minor repairs;

$60 > D_r \geq 40$: Class III, need for repair, and appropriate traffic control

$40 > D_r$: Class V. or IV

According to Highway Bridges and Culverts Specification "(JTG H11-2004) [12], the important component of worst defect level of technical condition is the evaluation criteria of control bridge condition.

The maximum width vertical cracks occurred at the mid span ($L/2$) near the longitudinal reinforcement was around of 0.25 mm, while the maximum width of diagonal cracks at the end has reached 0.3mm. The flange of beam have a local vertical and horizontal structural cracks, steel corroded and concrete cove has fall off; the foundation of the pier have leakage at the river bed about 50cm and bridge on the downstream riverbed dredging cause serious foundation erosion phenomenon. Due to increase in the traffic load and riverbed sand-digging, and the possibility of further developing the damages listed above, therefore, the bridge has a certain degree of

safety risks. The comprehensive assessment of the technical condition of the bridge was class III, it is recommended that as soon as possible to implement effective reinforcement and repair.

3.9 Bridge Structure Inspection

This inspection is based on the Reinforced Concrete and Pre-stressed Concrete Highway Bridge Design Specifications (JTJ023-85) [13] and Highway Bridges Carrying Capacity Detection Assessment Procedures of Zhong Xing Bridge reinforced concrete structure inspection.

In accordance with Highway Bridges and Culverts Standard Specifications (1973), the upper bridge structure is prefabricated reinforced concrete T-shaped beam bridge superstructure with 20m span, the standard drawings and design considered the main beam concrete grade is equivalent to 4 and type C25, the longitudinal reinforcement 12φ32mm and a 6φ28mm class II reinforced, is equivalent to type HRB335. The bridge design load class: Vehicle No. -15, and truck-80; pedestrian load loads: 3.0 kN/m². The total applied dead load 40.96 kN/m.

3.9.1 Lateral Distribution Coefficient.

Zhong Xing Bridge is prefabricated simply supported reinforced concrete T-Beam as a main girder span; four diaphragms beam each of the main beams between provide a good lateral stiffness of connection. The wide-span ratio of load-bearing structure is 0.41, less than 0.5, is a narrow bridge. It can be corrected eccentric pressure method in the cross-section of the main beam transverse distribution coefficient. After calculation, beam cross-section transverse load distribution coefficients are shown in Table 9:

Table 9 Transverse load distribution coefficients

| Item | Main beam | Mid-span section | Pier section |
|------------|------------|------------------|--------------|
| Vehicle-15 | Beam No. 1 | 0.823 | 0.700 |
| | Beam No. 2 | 0.667 | 0.968 |
| | Beam No. 3 | 0.823 | 0.700 |
| Truck -80 | Beam No. 1 | 0.496 | 0.399 |
| | Beam No. 2 | 0.333 | 0.700 |
| | Beam No. 3 | 0.496 | 0.399 |

In accordance with (Chinese Specification 85) "live load impact coefficient $\mu = 0.191$.

3.9.2 Live load internal force calculation results

Accordance with specification 85 [13], calculated live load of vehicle-15, Truck -80 and pedestrian load of cross section force, are shown in Table 10, Table 11 and Table 12 respectively.

Table 10 Live load internal force calculation results of different load levels.

| Item | Span moment M (kN.m) | | Beam end shear Q (kN) |
|-----------------|----------------------|------|-----------------------|
| vehicle-15 | M (max.) | 897 | 184 |
| | Q (max.) | 712 | 196 |
| Truck -80 | M (max.) | 1230 | 258 |
| | Q (max.) | 1130 | 272 |
| Pedestrian load | M (max.) | 681 | 123 |
| | Q (max.) | 371 | 133 |

Based on the software analysis program and accordance with Chinese Specifications -85 ,the ultimate strength design of the bridge was check, the results are shown in Table 13 and Table 14.

Table 13 Mid span stress calculation results (unit: MPa)

| Item (height) (m) | Stress | Maximum compressive stress | Maximum tensile stress | Maximum shear stress | Minimum shear stress | Maximum principal Stress | Maximum principal tensile stress |
|-------------------------|--------------------------|----------------------------------|------------------------------|----------------------------|----------------------------|--------------------------------|---|
| 1 (1.7) | Normal positive Stress | 3.82 | 3.82 | 0.0 | 0.0 | 3.78 | 0.00 |
| | Vertical positive stress | 0 | 0 | 0 | 0 | 0 | 0 |
| | Shear stress | 0 | 0 | 0 | 0 | 0 | 0 |
| | Principal | 3.82 | 3.82 | 0.0 | 0.0 | 3.78 | 0.0 |

| | | | | | | |
|---------------------|------------------------------|------|-----|------------------------|------------------------|------------------------|
| | compressive stress | | | | | |
| | Principal tensile stress | 0 | 0 | 0 | 0 | 0 |
| | Allowable value | 14.0 | 0 | 0 | 0 | -2.47 |
| | Whether acceptable | Yes | Yes | Yes | Yes | Yes |
| 2 (1.27) | Normal Positive Stress | 0 | 0 | 0 | 3.78 | 0 |
| | Vertical Positive Stress | 0 | 0 | 0 | 0 | 0 |
| | Shear stress | 0 | 0 | 0.102 | 0.102 | 0.102 |
| | Principal compressive stress | 0 | 0 | 0.102 | 0.102 | 0.102 |
| | Principal tensile stress | 0 | 0 | -0.102 | -0.102 | -0.102 |
| | Allowable value | 14 | 0 | 0 | 0 | -2.47 |
| | Whether acceptable | Yes | Yes | Yes | Yes | Yes |
| 3 (0.85) | Normal Positive Stress | 0 | 0 | 0 | 3.78 | 0 |
| | Vertical Positive Stress | 0 | 0 | 0 | 0 | 0 |
| | Shear stress | 0 | 0 | 0.102 | 0.102 | 0.102 |
| | Principal compressive stress | 0 | 0 | 0.102 | 0.102 | 0.102 |
| | Principal tensile stress | 0 | 0 | -0.102 | -0.102 | -0.102 |
| | Allowable value | 14 | 0 | 0 | 0 | -2.47 |
| | Whether acceptable | yes | yes | yes | yes | yes |
| 4 (0.425) | Normal positive Stress | 0 | 0 | 0 | 3.78 | 0 |
| | Vertical positive Stress | 0 | 0 | 0 | 0 | 0 |
| | Shear stress | 0 | 0 | 9.06×10^{-2} | 9.06×10^{-2} | 9.06×10^{-2} |
| | Principal compressive stress | 0 | 0 | 9.06×10^{-2} | 9.06×10^{-2} | 9.06×10^{-2} |
| | Principal tensile stress | 0 | 0 | -9.06×10^{-2} | -9.06×10^{-2} | -9.06×10^{-2} |
| | Allowable value | 14.0 | 0 | 0 | 0 | -2.47 |
| | Whether acceptable | Yes | Yes | Yes | Yes | Yes |
| 5 (0.0) | Normal Positive Stress | 0 | 0 | 0 | 0 | 0 |
| | Vertical Positive Stress | 0 | 0 | 0 | 0 | 0 |
| | Shear stress | 0 | 0 | 0 | 0 | 0 |
| | Principal compressive stress | 0 | 0 | 0 | 0 | 0 |
| | Principal tensile stress | 0 | 0 | 0 | 0 | 0 |
| | Allowable value | 14 | 0 | 0 | 0 | -2.47 |
| | Whether acceptable | Yes | Yes | Yes | Yes | Yes |

Table 14 ultimate strength section results checking (combination I)

| Item | Maximum axial force | Minimum axial force | Maximum bending moment | Minimum bending moment |
|-----------------------------------|-----------------------|-----------------------|------------------------|------------------------|
| Q_j (kN) | 0 | 0 | 0 | 0 |
| N_j (kN) | -0.69 | -0.69 | -90.5 | -0.692 |
| M_j (kN.m) | 2.3×10^3 | 2.3×10^3 | 4.72×10^3 | 4.72×10^3 |
| Force nature | Sagging | Sagging | Sagging | Sagging |
| R (kN.m) | 4.82×10^3 | 4.82×10^3 | 4.82×10^3 | 4.82×10^3 |
| Whether acceptable | yes | yes | yes | yes |
| Reinforcement area | 1.33×10^{-2} | 1.33×10^{-2} | 1.33×10^{-2} | 1.33×10^{-2} |
| Minimum reinforcement area | 5.97×10^{-4} | 5.97×10^{-4} | 5.97×10^{-4} | 5.97×10^{-4} |
| Whether acceptable | yes | yes | yes | yes |

Table 15 Ultimate strength section results checking (combination II)

| Position | Item | The upper edge of tension | The lower edge of tension |
|------------------------|-------------------------|---------------------------|---------------------------|
| Midspan section | Long-term Moment (kN.m) | 0 | 1.92×10^3 |
| | Full load moment(kN.m) | 0 | 3.64×10^3 |
| | Crack width limits (mm) | 0.2 | 0.2 |
| | Long-term crack (mm) | 0 | 0.172 |
| | Meets the requirements | yes | yes |

From Table 15 the above results indicate that the main beam meets the design requirements of specification-85 (truck -15 and Truck -80 levels).

3.10. Loading test program

Theoretical analysis of the identified bridge superstructure was based on the truck -80 level control designs as a standard test load.

The test loads used as the experimental load were two heavy-duty carrying timber vehicles, as shown in Fig. 24 and Fig. 25.

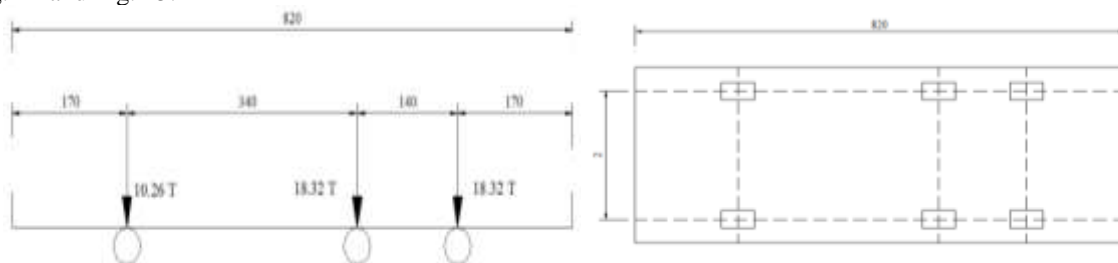


Fig. 24 Load schematic diagram test vehicles (black A7)
(Unit: cm, ton)

3.10.1 Cross-section strain measuring points

Strain measuring of main beam points arrangements are shown in Fig. 28.

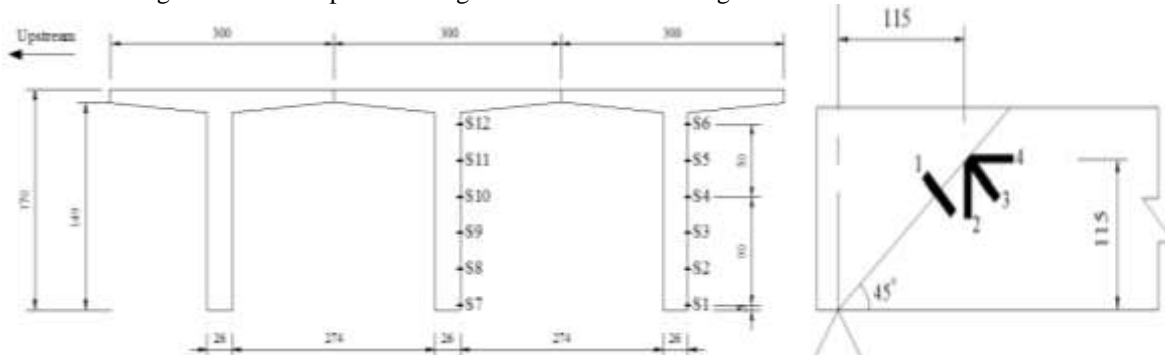


Fig. 28 Cross-section strain measurements point layout

Beam end-sectional strain measuring points shown in Fig. 29. The settlement in the upstream and downstream just above the pier (at the top curbs) was chooses.

3.10.2 Load conditions and load layout

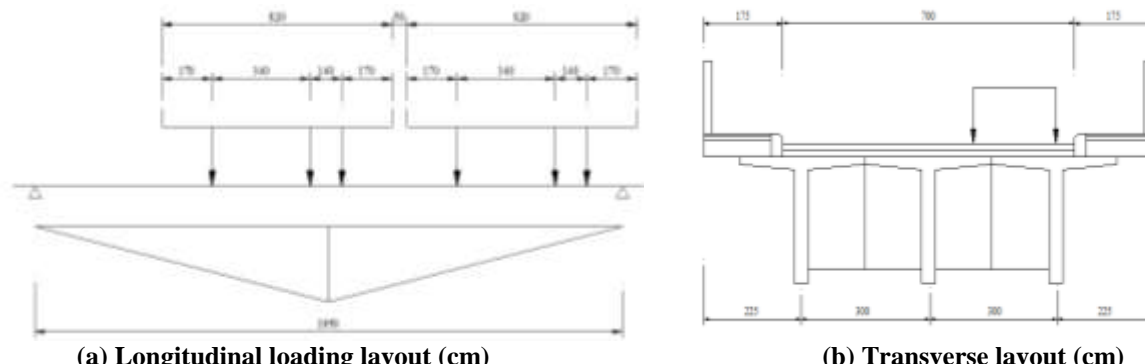
The loading test cases are shown in Table 16, to perform the static load analysis of Zhong Xing Bridge.

Table 16 Loading case detail

| Item | Loading conditions | Detect details. |
|------------|-----------------------------|---|
| I | Side beam middle span | deflection and concrete strain of the side beam |
| II | Middle beam Mid-span | deflection and concrete strain of mid span beam |
| III | Edge Beam Shear | maximum shear beam ends -Edge beam - |
| IV | Shear Middle-Beam | maximum shear at the end beam |
| V | Eccentric Pressure at Basis | Foundation Settlement |
| VI | Pure Pressure at Basis | Foundation Settlement |

3.10.3 Load position

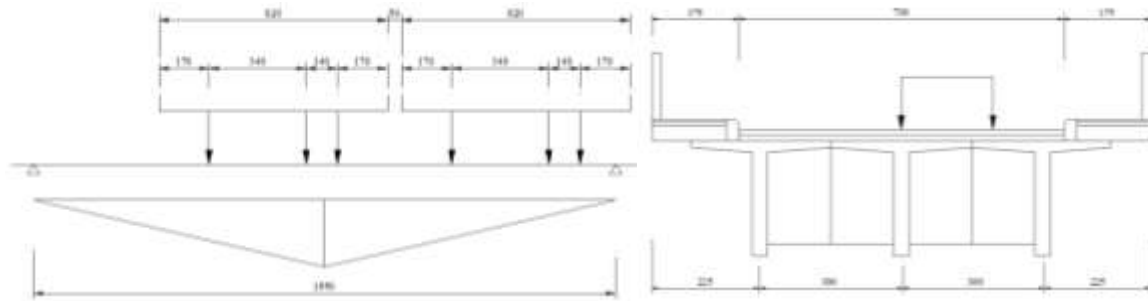
Various conditions in the load test arrangement are shown in Fig. 31.



(a) Longitudinal loading layout (cm)

(b) Transverse layout (cm)

Fig. 31 Loading Case I conditions test layout.



(a) Longitudinal loading layout (m)

(b) Transverse layout (cm)

Fig. 32 Loading Case II conditions test layout.

3.11. Test load efficiency

The full static load test was carried out to evaluate the efficiency of static loads, static load test efficiency η_q may calculate according to the following formula:

$$\eta_q = \frac{S_s}{S(1 + \mu)}$$

Where:

η_q : Static load test efficiency.

S_s : Calculated control section internal forces under static load;

S : Calculated control section internal forces under design loads.

μ : Calculated impact coefficient according to the design specification.

The comparison of test load and standard load effects on main beam control cross-section, the results are listed in Table 17.

Table 17 Conditions test load efficiency

| Case | Control Section Analysis | | | Impact factor (= 0.191) | Load efficiency η_g |
|------|--------------------------|--------------------------------------|--------------------------|----------------------------|--------------------------------|
| | Item Contents | Load test value (S _s) | Design calculated (S) | | |
| I | M(kN.m) | 1626 | 1920 | Included | 0.85 |
| II | M(kN.m) | 858 | 996 | Included | 0.86 |
| III | Q (kN) | 388 | 390 | Included | 0.99 |
| IV | Q (kN) | 205 | 218 | Included | 0.94 |
| VI | R (kN) | 663 | 656 | Not Included | 1.01 |
| V | R (kN) | 746 | 752 | Not Included | 0.99 |

3.12. Side Beam Cross-Section Deflection Test Results

In the case I test loads and from the main beam settlement value, the bearings and foundation deformation value can be obtained by the measured value of the side beam cross-section deflection. The comparison of theoretical calculation and the test results are shown in Table 18

Table 18 Mid-span deflection values of case I of the main beam under test loads

| Beam No. | Theoretical Value (mm) | Experimental Value(mm) | Calibration coefficient (Experimental/ Theoretical value) |
|----------|---------------------------|---------------------------|--|
| 1 | 9.7 | 6.26 | 0.65 |
| 2 | 5.2 | 3.53 | 0.68 |
| 3 | 0.8 | 0.67 | 0.84 |

The test results show that in the case I the test main beam deflection under the test load not only are less than their respective theoretical calculation results, also And the maximum value of the calibration factor of the respective main beam is 0.8.

Highway Bridge Carrying Capacity Detect Assessment Standard Procedures shows that the reinforced concrete beam bridge deflection calibration coefficient under common value within the range of from 0.6 - 0.9.

Reinforced concrete beam bridge deflection calibration coefficient under common Value within the range of from 0.6 to 0.9, note that each main beam has a certain degree of stiffness, to meet the use of the technical requirements for the design load.

3.13. Relative Residual Deformation.

The flexible of relative residual deformation as indicator of the performance structure to withstand the loads, relative residual of deflection deformation of each main beam span value is small. The degree of structure in the elastic state was insufficient.

Relative residual deformation S'_p can be calculated based on the following formula and its results are shown in Table 19

$$S'_p = \left(\frac{S_p}{S_t} \right) \times 100\%$$

Where:

S_p : Span deflection residual deformation.

S_t : Mid-span deflection.

Table 19 Deflection relative residual deformation results of main girder of case I

| Beam No. | Residual deformation (mm) | Measured Deformation (mm) | Relative residual deformation (%) |
|-------------|---------------------------------|---------------------------------|--------------------------------------|
| 1 | 0.23 | 6.26 | 3.7 |
| 2 | 0.17 | 3.53 | 4.8 |
| 3 | 0.06 | 0.67 | 9.0 |

From the Table 19, each main beam span deflection relative residual deformation under the loading test were less than 10%, indicating that the bridge structure elasticity in good working condition.

V. CONCLUSION

According to the load test, the following conclusions:

1. According to the test load results, the predict longitudinal strain of cross-section comparing with theoretical value, the calibration coefficient was between 0.724 - 0.896, and the average of 0.814, Test methods for long span bridges standard Requirements of calibration coefficient is between 0.70 - 0.90 range, the measured value of strain distribution along beam section height is less than the theoretical value, the test which explain that the beam structure have good performance.
2. From the test load results, the experimental vertical deflection values along the measurement point have varies from the calculated curved line, smooth longitudinal linear trend indicate that the stiffness of the structure, overall deformation, and integrity in good performance and working conditions. When loads are removed, the control section deformed basically restored to the initial state as before the applied the load, the residual deformation is very small, during the experiment the structure is always in flexible working state.
3. The vibration measured value of first order natural frequency is 3.7 Hz. The frequency measured value was greater than the theoretical value about 6%, the overall stiffness of Zhong Xing bridge meet the design requirement.
4. The observation of cracks in the body of each bridge pier showed there is no any the crack propagation and the piers work is normal.

In summary, the beams bridge carrying capacity and rigidity are meeting the Load level requirements of vehicle-15 level and Truck -80 levels.

VI. EVALUATION OF WHOLE BRIDGE STATE

The Zhong Xing Bridge has cracks in the main load-bearing structure, main beam concrete fall off, deck water leakage, cracks, exposed tendons and steel bar and pier foundation erosion exposed a variety of conditions.

In recent years with the increasing in traffic and heavy vehicles, riverbed sand erosion and other adverse factors lead to the possibility of further development of these problems.

According to the given above test results, the Zhong Xing Bridge Technical requirements already less than the original design requirement. In order to ensure the Zhong Xing Bridge safe operation and extended service life, it is recommended to take the following technical measurements:

5.1 Upper structure:

1. Strengthening of reinforced concrete T-beam to increase the carrying capacity of the bridge.
2. Because of the steel corrosion, concrete cracking and dropping parts, the appropriate patch must be carried out to spray with high toughness and anti-corrosion materials to improve the durability of the reinforced concrete structure.
3. Replacement of expansion joints. However, in order to improve traffic conditions, improve the bridge service levels, while the reducing workload of routine maintenance management, its recommend using a continuous deck structure as possible as to reduce the expansion joints.
4. Completely replace the waterproof layer, re-setting the pavement drain pipe and ensure that the drain pipe working well.
5. Re-laying of the bridge deck pavement. In order to reduce the bridge weight, it is recommended remove the original asphalt concrete overlay and then re apply the reinforced concrete pavement.
6. Re-laying of approach slab completely solve the bridgehead technical problems.

5.2 The Substructure Parts:

7. Re-paved bridge abutment the cone slope protection, reduce the wet period Washout Bridge station.
8. It is recommended to set a defense riverbed erosion dams, site about 10 to 20 meters of the bridge downstream dams and restore the riverbed height to the original status (cap top surface elevation +0.50 m) to overcome the technical problem effect on bridge pile cap Leakage.

ACKNOWLEDGEMENT

The authors are appreciative Heilongjiang Provincial Highway Administration and Harbin Institute of Technology School of Transportation Science and Engineering / Bridge and Tunnel Engineering (HIT) for the financial support, as well as technical staff of the laboratory to carry out the loading test.

REFERENCES

- [1]. Jaroslav Halvonik, Ming L. Wang and FanliFxu (2002), Health Assessment of Kishwaukee River Bridge"-Measurements in Advanced Materials and Systems.
- [2]. Doebling SW, Farrar CR, Prime MB. A summary review of vibration-based damage identification methods. Shock Vib Dig 1998;30(2):91-105.
- [3]. Lee JW, Kim JD, Yun CB, Yi JH, Shim JM, Health-monitoring. method for bridges under ordinary traffic loadings. J Sound Vibration 2002;257(2):247-64.
- [4]. Yam LH, Li YY, Wong WO. Sensitivity studies of parameters for damage detection of plate-like structures using static and dynamic approaches. Eng Struct 2002;24(11):1465-75.
- [5]. Kim H, Melhem H. Damage detection of structures by wavelet analysis. Eng Struct 2004; 26(3):347-62.
- [6]. Xu ZD, Wu ZS. Energy damage detection strategy based on acceleration responses for long-span bridge structures. Eng Struct 2007;29(4):609-17.
- [7]. Frangopol, D.M., Kong, J. and Gharaibeh, E. "Reliability-based life-cycle management of highway bridges", ASCE J. Comput. Civil Eng., 15(1), pp. 27–34 (2001).
- [8]. Suo, Q. and Stewart, M.G. "Corrosion cracking prediction updating of deteriorating RC structures using inspection information", Reliab. Eng. Syst. Saf., 94(8), pp. 1340–1348 (2009).
- [9]. Haleem K. Hussain, Lianzhen Zhang, Gui Wei Liu and Yongxue Li "Evaluation Behavior of Qing Shan Concrete Bridge under Static Load Test" Research Journal of Applied Sciences, Engineering and Technology 3(7): 677-688, 2011.
- [10]. Highway Engineering Technical Standards "(JTG B01-2003);
- [11]. Rebound Method of Concrete Compressive Strength Technical Specification, JGJ/T23-1992.
- [12]. Maintenance Highway Bridge and Culverts Specification JTG H11-2004.
- [13]. Reinforced Concrete and Pre-stressed Concrete Highway Bridge Design Specifications (JTJ023-85).